# Radial-homogeneous structures in nematic liquid crystals

**Alexander M. Parshin *[1,2], Victor Y. Zyryanov [1], and Vasily F. Shabanov [1]**

[1]Kirensky Institute of Physics, Federal Research Center KSC SB RAS, Krasnoyarsk, 660036, Russia
[2]Siberian Federal University, Krasnoyarsk, 660041, Russia
Correspondence and requests for materials should be addressed to A.M.P. (e-mail: parshin@iph.krasn.ru)

**Homogeneous nematic layers in liquid crystal cells with treated surfaces are affected by orientational transitions in the electric, magnetic, or temperature fields. The liquid crystal structures formed on solid or liquid surfaces find limited application in identifying the liquid-crystal states by the textures observed in polarized light. The use of surfaces prepared from polymer solutions makes it possible to significantly broaden the range of application of the liquid crystal structures, since they represent molecular formations stable at room temperature. The radial-homogeneous structures of the nematics formed by the polycarbonate surface in the presence of various residual solvents are investigated. The structures contained the disclination lines that aligned either by a glass plate rubbed to provide the homogeneous planar orientation in the LC layer or by a magnetic field applied along the polycarbonate film during the structure formation. The orientational transitions caused by surface treatment, temperature, and electric or magnetic fields in these structures are observed. The comparison of temperature critical distance as well as electric and magnetic coherence lengths with equilibrium length calculated from the expression for the free energy of the nematic is performed. Tricolor light transmission characteristics of structures as a function of electric field are obtained.**

## Introduction

Liquid crystals (LCs) in plane-parallel cells confined by solid surfaces have the homogeneous planar or homeotropic orientation or form the structures[1–6] that can be observed as various textures. Nematic LCs are characterized by the threaded, schlieren, and marbled textures. The textures typical of cholesteric, smectic, or discotic LCs are focal conic, polygonal, fan-shaped, and mosaic. The homogeneous nematic layers formed in cells with treated surfaces are involved in the temperature- and field-induced orientational effects, including the Fredericks or local Fredericks transition[7,8]. The structures allow the LC states[3] to be identified via texture observation in polarized light. The use of these structures in the orientational transitions is complicated by the uncontrollable conditions of director field distribution in an LC layer. The controlled conditions can be established in the nematic layers confined by non-solid surfaces with structural formations in the form of isotropic liquid droplets[9,10] or domains on the point defect network on the free LC surface[11–13]. However, the necessity in special preparation techniques and existence in the temperature range close to the nematic−isotropic liquid transition make these structures even more difficult to apply.

The use of polymer solution coatings in LC cells allows significant broadening of the range of application of the LC structures, which are molecular formations stable at room temperature. In particular, application of a magnetic field to a nematic LC layer during preparation of a polymer film by evaporation of a solvent from the polyvinylbutyral solution yielded homogeneous structures[14], which were then studied in the Fredericks transitions. Upon adsorption of nematic molecules on polycarbonate (PC) macromolecules in the presence of a residual solvent, a domain network occurred on the polymer film and continuously transformed to the homogeneous planar orientation over the nematic layer thickness[15]. In this study, we investigate the radial-homogeneous structures with the controlled director field distribution in the LC layer and a new nematic texture. The structures are formed and exist at room temperature,

undergoe the orientational transitions induced by surface treatment, temperature, and electric or magnetic fields, and can be considered as a promising soft organic material with the attractive physical, chemical, and optical properties.

## Materials and methods

**Materials.** As a polymer, we used a granular material synthesized from Bisphenol A carbonate (Sigma-Aldrich Co. LLC). The grains were dissolved in certain concentrations in one of the three solvents: dichloromethane $CH_2Cl_2$, chloroform $CHCl_3$, or pyridine $C_5H_5N$. The dichloromethane stabilized with ~ 20 ppm of amylene, chloroform stabilized with ~ 150 ppm of amylene and pyridine, 99% PS (Panreac Quimica S.L.U). As LCs, we used 4 metoxybenzylidene-4′-butylaniline (MBBA) and 4-n-pentyl-4′-cyanobiphenyl (5CB) nematics (both from Merck, Germany) with the phase transition sequences *Cr*–22°C–*N*–47°C–*I* and *Cr*–21.5°C–*N*–35°C–*I*, where *Cr* is the solid crystal, *N* is the nematic phase, and *I* is the isotropic liquid.

**Methods.** The LC structures were formed under interaction of nematics with the PC surfaces by evaporates of residual solvent prom the polymer film. The preparation conditions are given in Table 1. The polymer solution was deposited onto a glass surface by centrifuging and dried at a temperature of $t$ = 24°C for 1 min or annealed in a furnace at temperatures of $t_a$ = 50 or 120°C for 15 min. At the solvent evaporation for several seconds with average evaporating rate 40%/min, a PC film formed on the glass surface. The film thickness was from 100 nm to few microns up 0.4% (Filmetric F50-UVX). The nematics were deposited onto the polymer film at a temperature of $t_d$ = 24 or 30°C.

The nematic textures were studied using a polarized light microscope (Olympus BX51, Japan). Micrographs were done by camera (Micropublisher 3.3.RTR, Canada). The temperature for the samples preparation and investigations were controlled up ± 0.1°C (Linkam LTS120, UK). For alignment disclination lines the dc magnetic field $H^*$ up to 20 kOe was applied to the cell during the formation of the structure and was generated by an electromagnet.

To obtain the tricolor and volt-contrast characteristics, two types of LC cells formed on the basis of sample 15 (Table 1) with two glass plates were formed. In both cells, the bottom substrate was a glass plate coated with a conducting ITO layer and PC film. The film placed two Teflon spacers and the top glass plate with the ITO coating. In the first-type cell (RPP cell) the upper plate was rubbed. In the second-type cell (RPH cell) top plate was coated with the 1% solution of lecithin to obtain homeotropic alignment. In both cells, the LC layer thickness was $\delta$ = 30 μm. The cells was placed at the path of a He-Ne laser (R-39727, Newport, USA) beam with a wavelength of $\lambda$ = 633 nm. The voltage $U$ from the generator at 1 kHz was applied to the LC cell perpendicular to the surfaces and slowly scanned.

## Results and Discussion

**Nematic textures.** Fig. 1 shows the textures obtained under various preparation conditions. At low (below 0.6 wt.%) polymer concentrations and, correspondingly, high (over 99.4 wt.%) solvent concentrations, the nematics deposited at a temperature of $t_d$ = 24°C onto a polymer film dried at the same temperature, form the schlieren, threaded, or "grain-shaped" texture (Fig. 1(a)). The grain-shaped and "entangled thread-like" textures (Fig. 1(b)) are formed also upon annealing of the polymer film at temperatures of $t_a$ = 50 for 15 min. At temperatures of $t_a$ = 120°C for 15 min. the "island-shaped texture" (Fig. 1(c)) is formed. The texture formed in the nematics at polymer concentrations over 0.6 wt.% and, correspondingly, $CH_2Cl_2$ or $CHCl_3$ solvent concentrations below 99.4 wt.% at $t_a$ = 24°C and $t_d$ = 24°C resembles a polygonal texture observed in smectics. This *nematic polygon texture* (Fig. 1(d–h) did not form at any preparation conditions when the $C_5H_5N$ solvent was used. It should be noted that the textures shown in Figs. 1(a–c) occur for no more than 1 min after deposition of a nematic onto the PC film, while the nematic polygonal texture forms for a long time during the domain growth from nuclei

(Fig. 1(d)). The nuclei spontaneously arise on the PC film and increase proportionally to growth time τ, which depends on the polymer and solvent concentrations and temperature $t_d$ of LC deposition onto the polymer film. At a PC concentration of up to 1 wt.%, the entire domain ensemble forms for τ ≈ 10–15 min at $t_a$ = 24°C and $t_d$ = 24°C and the average domain size attains $d$ ≈ 70–150 μm (Fig. 2). An increase in the PC concentration to 3 wt.% leads to an increase in the growth time to τ ≈ 30–40 min and in the domain size to $d$ ≈ 150–200 μm. The dependence of the domain size on the PC concentration is caused by the physicochemical processes that occur at the PC/LC interface. Owing to the extinction, the nematic pulls the residual solvent from the polymer film to its boundary, where the mobility of polymer chains increases and the interaction between PC macromolecules and nematic molecules is intensified. The residual solvent concentration in the PC film determines the frequency of formation of nuclei and their growth slows down as domains touch one another. At the high (over 3 wt.%) polymer concentration, domains become coarse ($d$ ≈ 200 μm); however, the low mobility of polymer chains leads to the nonhomogeneous filling of the polymer film surface; i.e., the polymer material appears insufficient to form a high-quality polygonal nematic texture.

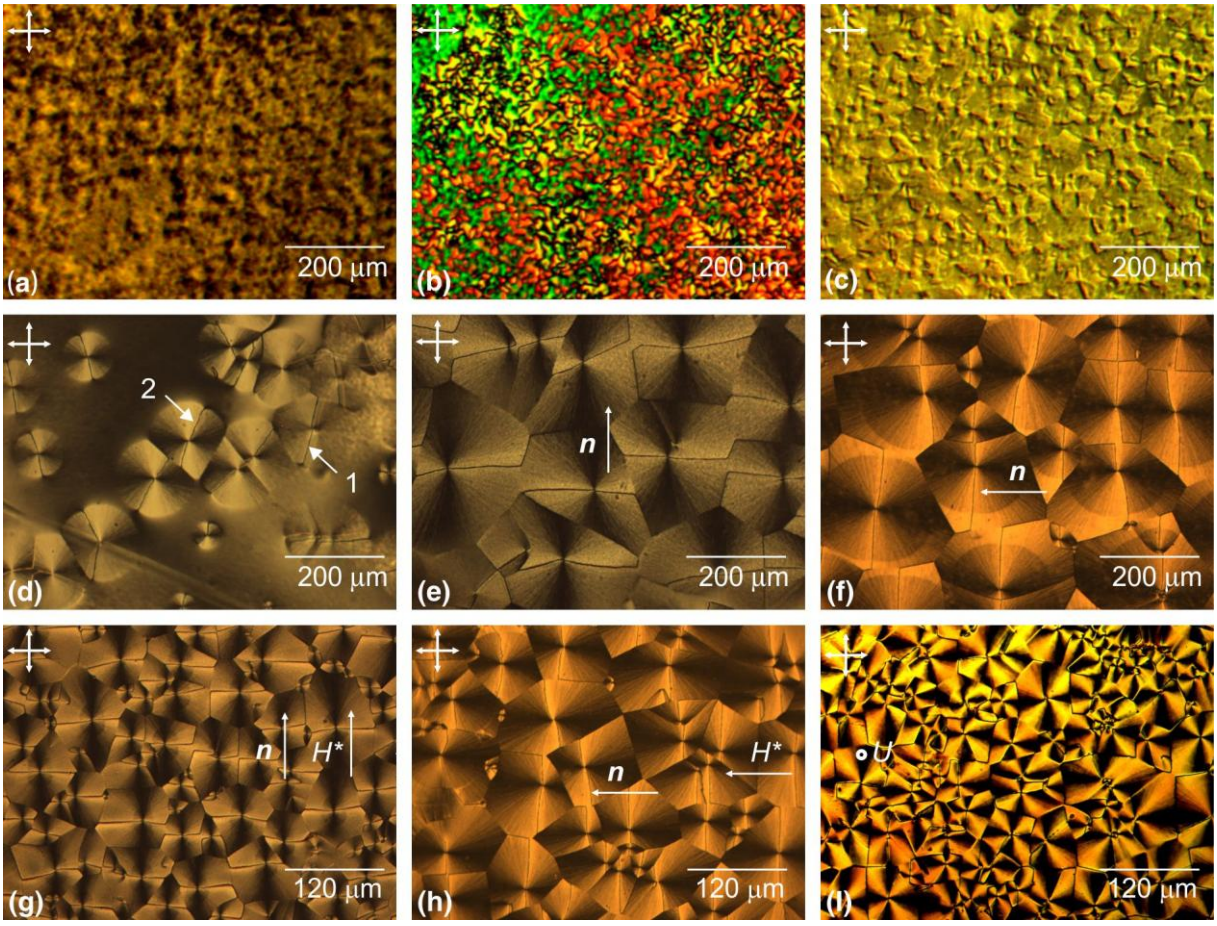


**Figure 1. Polarizing optical microphotographs of nematic textures**. **(a)** Sample 7: 1% of PC, $t_a$ = 50°C, $t_d$ = 24°C, and τ = 1 min. **(b)** Sample 8: 1% of PC, $t_a$ = 50°C, $t_d$ = 24°C, and τ = 1 min. **(c)** Sample 10: 1% of PC, $t_a$ = 120°C, $t_d$ = 24°C, and τ = 1 min. **(d)** Sample 12: 1% of PC, $t_a$ = 24°C, $t_d$ = 24°C, and τ = 7 min. **(e)** Sample 16: 2% of PC, $t_a$ = 24°C, $t_d$ = 24°C, and τ = 20 min. **(f)** Sample 20: 3% of PC, $t_a$ = 24°C, $t_d$ = 30°C, τ = 5 min. **(g)** Sample 16: 2% of PC, $t_a$ = 24°C, $t_d$ = 24°C, and τ = 20 min in a magnetic field of $H^*$ = 20 kOe applied in the PC film plane during the texture formation. **(h)** Sample 18: 2% of PC, $t_a$ = 24°C, $t_d$ = 24°C, τ = 35 min. **(i)** The "nematic fan texture" obtained from the "nematic polygonal texture" by the electric voltage of $U$ = 8.5 V applied perpendicular to the 30-μm-thick LC layer. The director of nematics is **n**. Arrows show the polarization direction.

An individual texture domain can be observed in crossed polarizers as a region with double extinction bands. Each domain is divided in two equal or unequal parts by a disclination line passing through its center, which is almost straight along the domain radius. At a certain position of the polarizers, the disclination lines can be seen Fig. 1(d) as thin dark lines 1 or broad bright lines 2. Under synchronous rotation of crossed polarizers, the thin dark lines broaden to $b \sim 10$ μm and brighten. If, during the polygon texture formation, we cover the PC film by a glass plate rubbed to provide the homogeneous planar orientation in the LC layer, the disclination lines will tend to align perpendicular to the rubbing direction. The degree of their alignment depends on nematic layer thickness ξ. At $\xi \approx 10$ μm, only a small part of the disclination lines will be aligned, while at $\xi \approx 2$ μm, all the lines will be oriented (Fig. 1(e,f)). Their orientation is similar to that obtained in magnetic field $H^*$ applied along the PC film during the structure formation. At $H^* = 2.5$ kOe only a part of the disclination lines will be aligned. At $H^* = 20$ kOe we can observe the total alignment of the disclination lines perpendicular to $H^*$ (Fig. 1(g,h). In both cases, the director ***n*** of the volume layer of the LC tends to align perpendicular to the disclination lines.

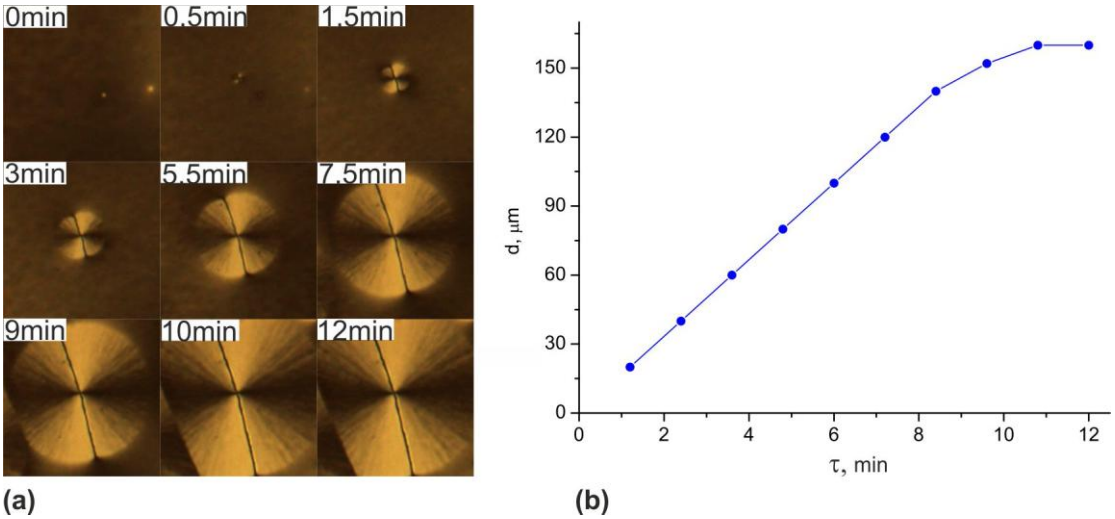


**Figure 2. Domain grows**. Sample 12: 1% of PC, $t_a = 24$°C, $t_d = 24$°C, and $\tau = 0 – 12$ min. (**a**) Micrographs of single domain. (**b**) Diameter *d* of single domain vs. τ.

If we cover the polygon texture by a glass plate treated in surfactants to provide the homogeneous homeotropic orientation, then at an LC layer thickness of $\xi \approx 3$ μm, the nematic polygonal texture will transform to the texture resembling the fan texture in cholesterics, smectics, or discotics. Similar transformation of the nematic polygonal texture to the *nematic fan texture* (Fig. 1(i)) occurs under the action of temperature or an electric or magnetic field applied perpendicular to the nematic layer. The temperature transition in MBBA and 5CB nematics starts with a temperature of $t_r = t - t_{NI} = 5.4$ °C, where $t_{NI}$ is the temperature of the nematic–isotropic liquid transition. During the transition, the sequential change in domain color from yellow to black at $t_r = t_{NI}$ is observed in crossed polarizers. The transition in the nematic layer with a thickness of $\xi \sim 30$ μm in an electric field occurred at a threshold voltage of $U_{th} = 1.6$ V and a magnetic field of $H_{th} = 1.5$ kOe and was also accompanied by the change in the texture color. At $U \sim 60$ V a dark field image was established in the LC cell.

An individual nematic fan texture domain is observed in crossed polarizers as a region with quadruple extinction bands (Fig. 3(a)). A point defect at the domain center has a force of $m = +1$, since under synchronous rotation of crossed polarizers the band rotation follows the light polarization directions and under sample rotation, they follow the direction opposite to sample rotation. If the LC is doped with a dye whose molecules are isomorphic to nematic molecules,

then the change in director $\boldsymbol{n}$ can be followed by the dye color change in one polarizer (Fig. 3(b–e)). The color is the brightest when the light polarization vector $\boldsymbol{e}$ coincides with the long axes of dye molecules and, consequently, with the nematic director $\boldsymbol{n}$ and the disclination line with length $l$ is maximally colored at $\boldsymbol{e} \perp l$ and brightens at $\boldsymbol{e} \parallel l$. This investigation shows that in the LC layer adjacent to the PC film, the director field configuration with three structural elements forms. During the growth, radial structure R of the nematic with director $\boldsymbol{n}_r$ forms on the PC surface (Fig 3(f)).

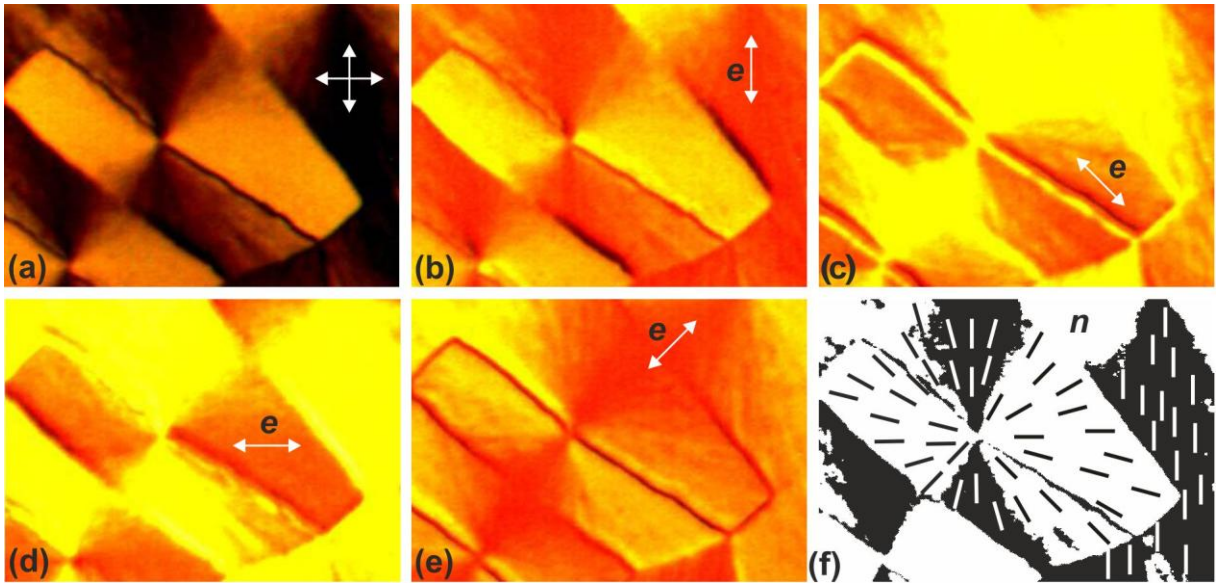


**Figure 3. Microphotographs of the dye-doped 5CB domain at certain angles of light polarization $\boldsymbol{e}$. (a)** In the crossed polarizers; (**b)** 0°;(**c)** 45°; **(d)** 90°; (**e)** -45°. **(f)** The director field configuration in the surface of domain.

The disclination line is a wall localized at the surface and fixed to the surface disclination line (SDL) with length $l$ similar to domain diameter $d$ and width $b$ at which the homogeneous distribution of director $\boldsymbol{n}_l$ perpendicular to $l$ is implemented. Under normal conditions, structure R would be unstable and the director would "escape" along the third dimension near the domain center[16]. However, the presence of the SDL stabilizes structure R. Owing to adsorption of LC molecules on polymer chains, R and SDL configurations are localized at the PC surface and a homogeneous planar or homeotropic bulk layer with director $\boldsymbol{n}_\mathbf{p}$ or $\boldsymbol{n}_\mathbf{h}$ forms over them. Various positions of directors $\boldsymbol{n}_r$, $\boldsymbol{n}_l$, and $\boldsymbol{n}_p$ or $\boldsymbol{n}_h$ lead to the existence of various stable nematic structures. When director $\boldsymbol{n}_l$ makes an angle with the polarization directions of light transmitted through polarizer $\boldsymbol{e}_p$ or analyzer $\boldsymbol{e}_a$, the SDL can be seen as a narrow dark line. When $\boldsymbol{n}_l$ is close to $\boldsymbol{e}_a$ or $\boldsymbol{e}_p$, the SDL remains narrow, but structure R can be seen as an area with double extinction bands. If the planar layer is superimposed on structure R, the area with double extinction bands is observed in crossed polarizers. If director $\boldsymbol{n}_l$ is close to $\boldsymbol{n}_\mathbf{p}$, as well as to $\boldsymbol{e}_a$ or $\boldsymbol{e}_p$, the SDL can be seen as a narrow dark line. When $\boldsymbol{n}_l$ makes an angle with $\boldsymbol{n}_\mathbf{p}$, the SDL is observed as a broad bright line.

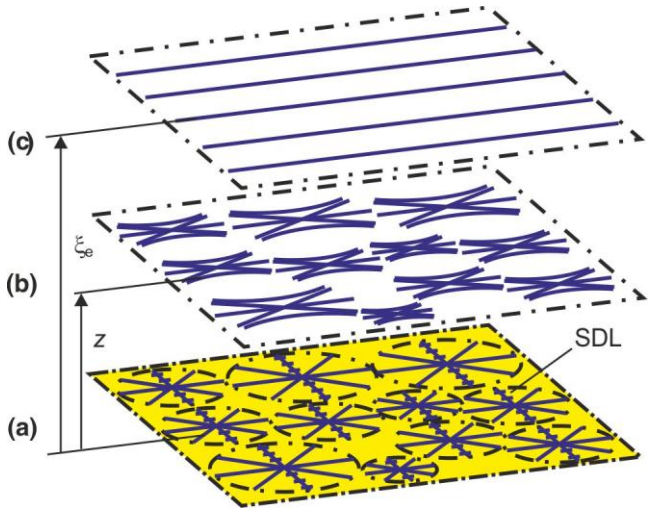


**Figure 4. Schematic of the radial-planar structure: on polycarbonate surface. (a)** At the PC film; **(b)** at a distance *z* from the surface; **(c)** at equilibrium length $\xi_e$.

**Structures of the nematic domains.** Fig. 4 shows a schematic of the radial planar (RP) structure with the SDL. Radial structure R with the SDL is concentrated on the polymer surface and continuously transforms to homogeneous planar structure P at equilibrium distance $\xi_e$ from the surface. Taking into account averaged elasticity constant *K*, we can express the free energy of the LC in volume *V* as[7]

$$F = \frac{1}{2} K \int_v [(\nabla \cdot \boldsymbol{n})^2 + (\nabla \times \boldsymbol{n})^2] dV. \quad (1)$$

For structure RP, the components of director ***n*** in the cylindrical system of coordinates *O*ρφ*z* are $n_\rho = -\cos\psi$, $n_\varphi = \cos\psi$, and $n_z = 0$, where ψ is the angle between director ***n*** and polar radius ρ. The angle of deviation of molecules from ρ on the surface with the molecular adsorption is ψ = 0 at *z* = 0 and ψ = φ at the distance *z* = ξ. Assuming the local distortion of the director field to decay exponentially from the surface[7] (ψ = (1–exp (–*z*/ξ)) φ and performing integration within $b/\cos\varphi \le \rho \le r$, $0 \le \varphi \le 2\pi - 4 \cdot \mathrm{asin}(b/\rho)$, $0 \le z \le \infty$, obtain

$$F_1 = \frac{1}{2} K \left[\pi \ln\left(\frac{2r}{b}\right) \xi + [\pi(\pi - 3) + 12] \frac{r^2}{24\xi} + \pi(\pi - 4) \frac{r}{4}\right] + F_l, \quad (2)$$

where *r* is the domain radius, *b* is the SDL width, and $F_l$ is the SDL energy. Minimization of (2) yields the equilibrium $\xi_e$ value

$$\xi_e = \left\{\frac{[\pi(\pi-3)+12]}{24\pi \ln\left(\frac{2r}{b}\right)}\right\}^{\frac{1}{2}} r. \quad (3)$$

The SDL is oriented by the rubbed plate or magnetic field $H^*$ during the structure formation via oriented molecules of the bulk LC layer. The LC molecules in the SDL are fixed to *l* due to adsorption and tend to rotate cooperatively under the action of molecular forces. In this case, the torque occurs that rotate the SDL perpendicular to the director of the homogeneous bulk LC layer. The torque value depends on the mobility of polymer chains and the critical equilibrium length, which, as experiment shows, is $\xi_c \approx 2$ μm. The magnetic coherence length[7] at a field of $H^* = 20$ kOe, magnetic susceptibility anisotropy of $\Delta\chi = 1.16 \cdot 10^{-7}$, and an elasticity constant of $K = 6 \cdot 10^{-7}$ dyn[17] is also $\xi_H = 1/H^*(K/\Delta\chi) \approx 2$ μm.

The transition from the nematic polygonal to nematic fan texture can occur when equilibrium length $\xi_e$ is equal to the coherence length of the external field. Assuming that structures R and SDL variously depend on temperature, their intersection at critical distance $\xi_t$ from the surface should lead to the temperature transition[8] at $\xi_t = \xi_e$. Approaching of the electric ($\xi_E$) or magnetic ($\xi_H$) coherence lengths to equilibrium length $\xi_e$ facilitates the orientational transition in an electric or magnetic field. Substituting the average domain radius $r \approx 55$ μm and $b \approx 10$ μm (Fig. 1(g)), we obtain from Eq. (3) the value of $\xi_e \approx 15$ μm, which is consistent with $\xi_H = 1/H\ (K/\Delta\chi) \approx 15$ μm at the experimental value of $H = 1.5$ kOe. At the same time, it is difficult to do estimates of the $\xi_t$ and $\xi_E$ values due to strong nonuniformity of the electric field in the LC with the strained transition layer with length $\xi_e$.

**Optical characteristics of the nematic structures in the electric field.**

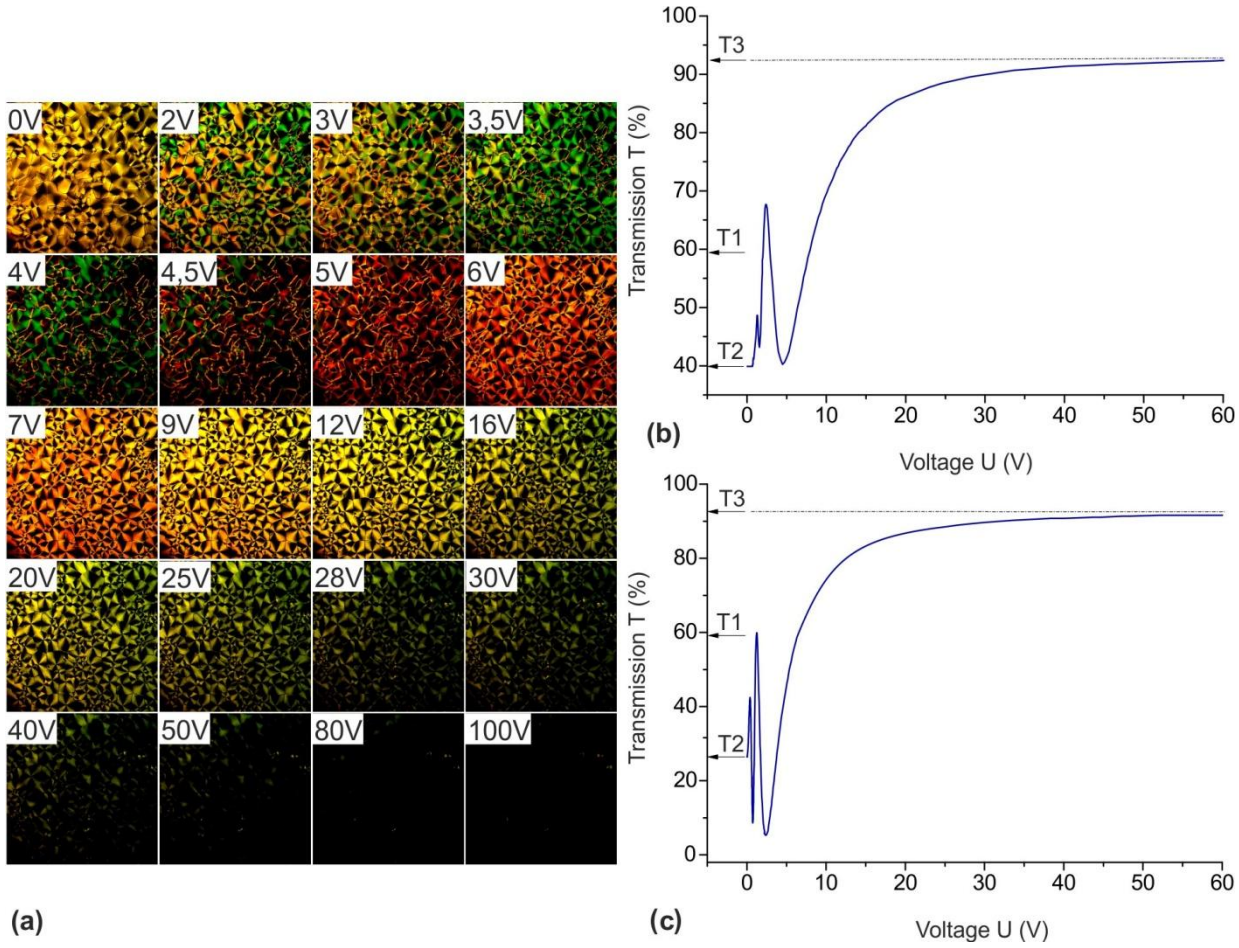


**Figure 5. The transition from the nematic polygonal to nematic fan texture**. (**a**) The micrographs of domains ensemble at various values *U*. (**b,c**) Monochromatic light transmission *T* vs. electric voltage *U*. Laser radiation was transmitted through a cell formed on the basis of sample 15 with the upper plate: (**b**) rubbed; (**c**) treated by surfactants.

Fig. 5 shows the volt-contrast characteristics $T(U)$ for the RP structure obtained with the use of monochromatic laser radiation in the absence of polarizers. In the RPP cell for structure formation time τ, transmission $T$ decreases from a value of $T_1 \approx 60\%$ corresponding to scattering of the nonhomogeneous structure with the threaded or schlieren texture to a value of $T_2 \approx 40\%$ corresponding to scattering of the RP structure. Then, if we apply a field of $H^* = 20$ kOe along the rubbing direction during the structure formation, transmission $T$ increases to a value of $T_1^* \approx 90\%$, which then decreases to $T_2$ due to the scattering for time τ. We observed the monotonic variation change of $T$ from $T_2$ to $T_3$, which corresponds to the transition of the RP

structure to the homeotropic state at a voltage of $U > 30$ V. The volt-contrast characteristic $T(U)$ is accompanied by interference maxima and minima, which can be attributed to the inhomogeneities caused by the R structure. The obtained optical characteristics are comparable with the characteristics of the PDLC structures[18,19] used in devices based on the light scattering phenomenon. The significant variations in $T$ observed in the RPH cell evidence for the stability of the RP structure, which remains unchanged at $\xi_H \geq \xi_e$ even at the competing effect of the upper plate in the LC cell.

Fig. 6 shows tricolor characteristics of light transmission of the RPP cell as a function of electric field. The cell was places between crossed polarizers and illuminated by normally incident white light transmitted through a red (R), green (G), or blue (B) filter with wavelengths of $\lambda(R) = 700$, $\lambda(G) = 520$, and $\lambda(B) = 452$ nm, respectively. It can be seen in Fig. 5 that there is a potential difference between extrema of curves R, G, and B, which is comparable with the differences obtained for hybrid-aligned nematic cells[20] or cells with color filters[21] used in multicolor LC displays.

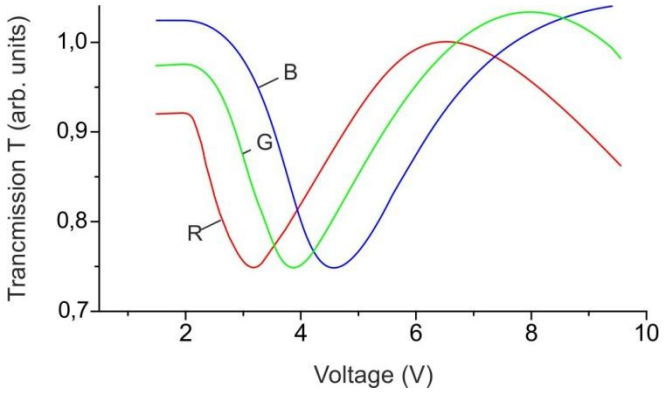


**Figure 6. White light transmission *T* of the LC layer vs. electric voltage *U*.** The light was transmitted through a cell formed on the basis of sample 15 using red (R), green (G), and blue (B) filters in crossed polarizers.

## Conclusion

Thus, the textures of the 5CB and MBBA nematics formed by the polycarbonate surface in the presence $CH_2Cl_2$, $CHCl_3$ or $C_5H_5N$ as new "grain-shaped", "entangled thread-like" or "polygonal" nematic textures were observed. The most attractive is the "polygonal" nematic texture that displays the radial-planar structure consisted of an ensemble of domains growth from nuclei. Each domain is divided in two equal or unequal parts by a disclination line with homogeneous molecular layer, which ensures stability of the radial configuration via preventing "escape" of the director along the third dimension. The disclination lines are aligned by a glass plate rubbed to provide the homogeneous planar orientation in the LC layer with a thickness of $\xi \approx 2$ μm and by a magnetic field of $H^* = 20$ kOe applied along the polycarbonate film during the structure formation. If we cover the radial-planar structure by a glass plate treated in surfactants to provide the homogeneous homeotropic orientation, then at an LC layer thickness of $\xi \approx 3$ μm, has been transformed to the radial-homeotropic structure. The similar transformation in the nematic layer with a thickness of $\xi \sim 30$ μm occurs at a temperature of $t_r = t - t_{NI} = 5.4$ °C, as well as in an electric field at a threshold voltage of $U_{th} = 1.6$ V or a magnetic field of $H = 1.5$ kOe, which are applied perpendicular to the nematic layer. The radial-planar structure is characterized by the equilibrium distance from the polymer surface $\xi_e$. When the critical temperature length $\xi_t$ and electric ($\xi_E$) or magnetic ($\xi_H$) coherence lengths approach $\xi_e$, the orientational transition from the radial-planar to homeotropic-planar structure occurs. In the tricolor characteristics of light transmission $T$ of radial-planar structure as a function of voltage $U$ there is a potential difference between extrema of red, green, and blue lights that could be used

in displays. The volt-contrast characteristics $T(U)$ are accompanied by interference maxima and minima. These phenomena can be used in displays and devices based on the light scattering.

## References


1. Friedel, G. Les etats mesomorphes de la matiere. *Ann. Phys*., **19**, 273–483 (1922).
2. Frank, F. C. On the theory of liquid crystals. *Discuss. Faraday Soc.* **25**, 19–28 (1958).
3. Sackmann, H., Demus, D. The Polymorphism of liquid crystals. *Mol. Cryst*. **2**, 81–102 (1966).
4. Nehring, J., Saupe, A. On the schlieren texture in nematic and smectic liquid crystals. *J. Chem. Soc. Far. Trans*. **II 68**, 1–15 (1972).
5. Dierking, I. *Textures of Liquid Crystal* (Wiley–VCN, Weinheim, Germany, 2003).
6. Kleman, M Lavrentovich, O. D. Topological point defects in nematic liquid crystals. *Phil. Mag*. **86**, 4117–4137 (2006).
7. De Gennes, P.G., Prost, J. *The Physics of Liquid crystals* 2nd edn (Clarendon Press, Oxford, 1993).
8. Dubois-Violette, E., de Gennes, P. G. Local Frederiks transition near a solid/nematic interface. *J. Phys.* **36**, L-255–L-258 (1975).
9. Meyer, R. B. Point disclinations at a nematic-isotropic liquid interface. *Mol. Cryst. Liq. Cryst*. **16**, 355–369 (1972).
10. Press, M. J.; Arrot, A. S. Theory and experiments on configurations with cylindrical symmetry in liquid-crystal droplets. *Phys. Rev. Lett*. **33**, 403–406 (1974).
11. De Gennes, P. Structures en domains dans un nematique sous champ magnetique. G. *Sol. State Commun*. **8**, 213-216 (1970).
12. Madhusudana, N. V.; Sumathy K. R. Orientations on nematic liquid crystal with an onlique orientation of the director at the nematic-isotropic interface. *Mol. Cryst. Liq. Cryst*. **129**, 137–147 (1985).
13. Lavrentovich, O. D.; Nastishin, Yu. A. Defects in degenerate hybrid aligned nematic liquid crystals. *Europhys. Lett.* **12**, 135–141 (1990).
14. Parshin, A. M. Gunyakov, V. A. Zyryanov, V. Ya., Shabanov. V. F. Magnetic-field-assisted formation of alignment polymer coatings in Liquid Crystal Cells. *Tech. Phys. Lett*. **34**, 571–573 (2008).
15. Parshin, A. M. Gunyakov V. A., Zyryanov V.Ya., Shabanov, V. F. Domain structures in nematic liquid crystals on the polycarbonate surface. *Int. J. Mol. Sci.* **14**, 16303–16320 (2013).
16. Meyer, R. B. On the extence of even indexed disclination in nematic liquid crystal. *Phil. Mag*. **27**, 405–424 (1973).
17. Parshin, A. M., Nazarov V. G., Zyryanov V. Ya., V.F. Shabanov. Magnetic-field-induced structural transition in polymer-dispersed liquid crystals. *Mol. Cryst. Liq. Cryst*. **557**, 50–59 (2012).
18. Margerum, J. D., Lackner, A. M., Ramos, E., Lim K.-C., et al. Effects off-state alignment in polymer dispersed liquid crystals. *Liq. Cryst*. **5**, 1477–1487 (1989).
19. Prishchepa, O. O., Parshin, A. M., Shabanov, A. V., Zyryanov, V. Ya. Magneto-optical study of Friedericksz threshold in polymer dispersed nematic liquid crystals. *Mol. Cryst. Liq. Cryst*. **488**, 309–316 (2008).
20. Matsumoto, S., Masahiro K., Kiyoshi M. Field-induced deformation of hybrid-aligned nematic liquid crystals: new multicolor liquid crystal display. J. Appl. Phys. **47**, 3842–3845 (1976).
21. Depp, S. W., Ong H. L. Multicolor liquid crystal display. US patent 4968120 A (1990).


## Acknowledgements


This work was supported by the Russian Foundation for Basic Research (project No. 15-02-06924 and No. 16-53-00073).

## Author Contributions

A. M. P. prepared samples, investigated their electro-optical and magneto-optical characteristics and performed the computational procedures. A. M. P. and V. Y. Z. reviewed the data and wrote the paper. V. F. S. checked, revised and finalized the paper.

## Additional information.

**Competing financial interests.** The authors declare that they have no competing financial interests.

| Sample no. | Polymer (wt. %) | Solwent (wt. %) | | | Liquid crystal | | Drying temperature (°C) | Deposition temperature (°C) | Shaping time (min) | Texture |
|---|---|---|---|---|---|---|---|---|---|---|
| | PC | $CH_2Cl_2$ | $CHCl_3$ | $C_5H_5N$ | MBBA | 5CB | $t_a$ | $t_d$ | τ | |
| 1 | 0.2 | 99.8 | | | ν | | 24 | 24 | 1 | t[a] |
| 2 | 0.2 | 99.8 | | | | ν | 24 | 24 | 1 | g[b] |
| 3 | 0.6 | 99.4 | | | ν | | 24 | 24 | 1 | g |
| 4 | 0.6 | 99.4 | | | | ν | 24 | 24 | 7 | g |
| 5 | 1 | | | 99 | ν | | 24 | 24 | 1 | g |
| 6 | 1 | | | 99 | | ν | 24 | 24 | 1 | g |
| 7 | 1 | 99 | | | ν | | 50 | 24 | 1 | e[c] |
| 8 | 1 | 99 | | | | ν | 50 | 24 | 1 | e |
| 9 | 1 | 99 | | | ν | | 120 | 24 | 1 | i[d] |
| 10 | 1 | 99 | | | | ν | 120 | 24 | 1 | i[d] |
| 11 | 1 | 99 | | | ν | | 24 | 24 | 15 | p[e] |
| 12 | 1 | 99 | | | ν | | 24 | 24 | 12 | p |
| 13 | 1 | | 99 | | | ν | 24 | 24 | 10 | p |
| 14 | 1 | | 99 | | | ν | 24 | 24 | 10 | p |
| 15 | 2 | 98 | | | | ν | 24 | 24 | 25 | p |
| 16 | 2 | 98 | | | ν | | 24 | 24 | 20 | p |
| 17 | 3 | 97 | | | ν | | 24 | 24 | 40 | p |
| 18 | 3 | 97 | | | | ν | 24 | 24 | 35 | p |
| 19 | 3 | 97 | | | ν | | 24 | 30 | 8 | p |
| 20 | 3 | 97 | | | | ν | 24 | 30 | 5 | p |

[a]Thread-likes texture. [b]Grain-shaped texture. [c]Enhangled thread-likes texture. [d]Island-shaped texture. [e]Polygon nematic texture

**Table 1. The preparation conditions and types of nematic textures on the polymer surface.**